Hierarchical Distributed MPC for Longitudinal and Lateral Vehicle Platoon Control with Collision Avoidance

Hankun Liu[1], Zhiwen Qiang[1], Li Dai*[1], Boli Chen[2], Yuanqing Xia[1]

1. Beijing Institute of Technology, Beijing 100080, China

2. University College London, London WC1E 6BT, UK

Abstract: This paper proposes a hierarchical distributed model predictive control (MPC) method for the vehicle platoon control in both longitudinal and lateral directions. In the upper layer, a novel path planning module and a trajectory-fusion module are utilized to compute a smooth reference trajectory for each follower. In the lower layer, the longitudinal and lateral distributed model predictive controllers are decoupled to control the velocity and steering respectively. To ensure safety and reduce the computation burden, the constraints to avoid collision are reformulated by using the strong duality theory. A simulation is conducted to demonstrate the effectiveness of the proposed control algorithm to maintain the platoon formation and to ensure the safety of the platoon.

Key Words: Distributed model predictive control, Longitudinal and lateral control, Vehicle platoon, Collision avoidance constraints

1 Introduction

The main objective of platoon control of each follower vehicle is to follow the leader vehicle and meanwhile maintain a comfortable/acceptable inter-vehicle distance. Many multi-vehicle platoon control mechanisms, including PID control, sliding model control (SMC), and model predictive control (MPC), have been proposed in the literature [1]. PID can be easily used in engineering [2–4]. To improve the performance of traditional PID control, a PID control method is proposed by adding acceleration of predecessor vehicle as feedforward information [3]. In [4], the velocity and position errors from the leader vehicle and predecessor vehicle are both introduced and utilized. However, these methods only work on the linear vehicle model, and vehicles are always nonlinear systems. SMC methods own strong robustness to deal with the external disturbance and model uncertainties, and thus have better performance on nonlinear vehicle model [5, 6]. However, the robustness will be degraded if there exists communication delay as pointed out in [7]. To maintain the satisfaction of safety constraints and physical constraints in a platoon, MPC has been widely applied in platoon control for its ability to theoretically handle diverse constraints [8–11].

In [8], the vehicle model is decoupled and a coupled cost function is designed, which reduces the computation burden compared with coupled vehicle models. In [10], a distributed MPC method is proposed for vehicle platoon and the effectiveness is demonstrated by a vehicular experiment. The authors in [11] develop a distributed MPC method to control the platoon under different unidirectional communication topologies. However, most existing researches on platoon control focus on the formation of vehicles in the longitudinal direction, and ignore the influence of steering. The lateral platoon control is significant in forcing the follower vehicles driving along a certain vehicle lane, or reforming the formation. There are mainly two sorts of methods for the lateral platoon control, following the road or following the vehicle. The former one is always more dependent on the road infrastructure. In the Program on Advanced Technology for the Highway (PATH) [12], the lateral control is completed by installing magnetic markers along the road. Recent studies [13, 14] are more expensive in finance due to the huge and complex infrastructure demands. As a result, the vehicle-following method is regarded as a more acceptable way in economic consideration. A vehicle-following framework including a path estimation method is proposed in [15], which is able to control the follower vehicles to follow the path of leader. In [16], a novel vehicle-following method is raised to compute a feasible following path for each follower vehicle by recording and resampling the path of the predecessor vehicle. However, due to the complicity of the vehicle model and the heavy computation burden, the safety issue of the platoon is not taken into consideration.

In this paper, we propose a hierarchical distributed MPC framework for platoon control. The control target of each follower in the platoon is to follow the leader if no obstacle is detected, and circumambulate the obstacles to avoid collision if obstacles are detected. The upper layer of each follower vehicle will receive the information from the predecessor vehicle, detect the environment surrounding local vehicle, and give a smooth feasible path by using a novel path planning algorithm. Besides, a combined reference trajectory can be computed based on the planned path and the information from the predecessor vehicle in the upper layer. Then, the local follower vehicle can be controlled to follow the platoon and bypass obstacles under the proposed distributed MPC control algorithm in the lower layer controller. To reduce the computation burden, the safety constraints calculated in the lower layer controller is reformulated by utilizing the strong duality theory.

Notation: Define 2-norm of vector x as $\|x\| = \sqrt{x^\top x}$ and $\|x\|_Q$ as $\|x\|_Q = \sqrt{x^\top Q x}$. $\|x\|_*$ denotes the dual norm of x. Given set $\mathcal{A}$ and $\mathcal{B}$, $\mathcal{A}\backslash\mathcal{B}$ denotes $\{j : j \in \mathcal{A}, j \notin \mathcal{B}\}$. Denote Minkowski sum $\mathcal{C}$ of set $\mathcal{A}$ and set $\mathcal{B}$ as $\mathcal{C} = \mathcal{A} \bigoplus \mathcal{B} = \{c : c = a + b, a \in \mathcal{A}, b \in \mathcal{B}\}$.

2 Problem Formulation

Consider a vehicle platoon consisting of a leader vehicle with subscript 0 and N follower vehicles indexed by

This work was supported by the National Natural Science Foundation of China under Grant 62173036 and Grant 62122014.

$1, 2, \ldots, N$ in order. Denote $\mathcal{N}_+ = \{1, 2, \ldots, N\}$.

2.1 Longitudinal Model

This paper assumes that the influence of the aerodynamic drag can be ignored and the driving and braking torques can be integrated in a first-order differential system. Then the longitudinal dynamics of each follower vehicle i, $i \in \mathcal{N}_+$ can be modelled as [11]

$$\begin{cases} x_i(t+1) = x_i(t) + v_i(t)\Delta t \\ v_i(t+1) = v_i(t) + \dfrac{\Delta t}{m_i}\left(\dfrac{\eta_{T,i}}{R_i}T_i(t) - m_i g \mu_i\right) \\ T_i(t+1) = T_i(t) + \dfrac{\Delta t}{\tau_i}\left(u_{ix}(t) - T_i(t)\right) \end{cases}, \quad (1)$$

where x_i and v_i denote the longitudinal position and velocity of follower vehicle i respectively; Δt is the discrete time interval; m_i represents the vehicle mass; $\eta_{T,i}$ denotes the transmission coefficient; R_i is the tire radius; g is the gravity constant; μ_i is the coefficient of rolling resistance; τ_i is the inertial lag of the longitudinal dynamics; T_i is the integrated accelerating/barking torque and u_{ix} is the control input.

By denoting $\xi_{ix}(t) = [x_i(t), v_i(t), T_i(t)]^\top$ and $\eta_{ix}(t) = [x_i(t), v_i(t)]^\top$ as the longitudinal state and output of vehicle i, $i \in \mathcal{N}_+$, the longitudinal dynamics (1) can be rewritten as

$$\begin{cases} \xi_{ix}(t+1) = f_{ix}(\xi_{ix}(t), u_{ix}(t)) \\ \eta_{ix}(t) = \gamma_x \xi_{ix}(t) \end{cases}, \quad (2)$$

with $\gamma_x = \begin{bmatrix} 1,0,0 \\ 0,1,0 \end{bmatrix}$.

To ensure the safety of the platoon and the physical limitations satisfaction, each follower vehicle is subject to the following constraints

$$u_{ix}(t) \in \mathbb{U}_{ix}, \quad (3)$$

$$v_i(t) \in \mathbb{V}_i, \quad (4)$$

$$x_{i-1}(t) - x_i(t) \geq d_{safe}, \quad (5)$$

where d_{safe} is the minimal safe distance between adjacent vehicles, and $\mathbb{U}_{ix}, \mathbb{V}_i$ are the longitudinal input and velocity constraints respectively.

2.2 Lateral Model

By utilizing Ackerman Turning Geometry Model, the suspension characters are ignored and the forces on the tires can be integrated into the midline of the vehicle. The lateral dynamics of each vehicle i, $i \in \mathcal{N}_+$ is given by

$$\begin{cases} m_i \ddot{x}_i = m_i \dot{y}_i \dot{\phi}_i + F_{i,xf} + F_{i,xr} \\ m_i \ddot{y}_i = -m_i \dot{x}_i \dot{\phi}_i + F_{i,yf} + F_{i,yr} \\ I_i \ddot{\phi}_i = l_{if} F_{i,yf} - l_{ir} F_{i,yr} \end{cases}, \quad (6)$$

where $\dot{y}_i$ denotes the lateral velocity; $\dot{x}_i = v_i$ denotes the longitudinal velocity; $\dot{\phi}_i$ is the yaw rate; $F_{i,xf}$, $F_{i,yf}$, $F_{i,xr}$ and $F_{i,yr}$ are respectively the projections of front tire force $F_{i,f}$ and rear tire force $F_{i,r}$ on x-axis and y-axis; l_{if} and l_{ir} are the front and rear wheel base respectively; and I_i is the moment of inertia.

Assume that the sideslip angles α_{if} and α_{ir} are small enough such that the complex tire forces $F_{i,yf}$ and $F_{i,yr}$ can be simplified as linear functions [17]

$$\begin{aligned} F_{i,yf} &= -C_{if}(\alpha_{if} - \delta_i), \\ F_{i,yr} &= -C_{ir}\alpha_{ir}, \end{aligned} \quad (7)$$

where the control input δ_i is the wheel steering angle, and C_{if} and C_{ir} are the tire sideslip rigidity coefficients. The sideslip angle α_{if} and α_{ir} can be calculated as

$$\begin{aligned} \alpha_{if} &= \arctan\frac{\dot{y}_i + l_{if}\dot{\phi}_i}{\dot{x}_i} \approx \frac{\dot{y}_i + l_{if}\dot{\phi}_i}{\dot{x}_i}, \\ \alpha_{ir} &= \arctan\frac{\dot{y}_i - l_{ir}\dot{\phi}_i}{\dot{x}_i} \approx \frac{\dot{y}_i - l_{ir}\dot{\phi}_i}{\dot{x}_i}. \end{aligned} \quad (8)$$

For vehicle i, the projections of the velocity $\dot{X}_i$ on X-axis and $\dot{Y}_i$ on Y-axis can be transformed from that in the vehicle body frame

$$\begin{aligned} \dot{X}_i &= \dot{x}_i \cos\phi_i - \dot{y}_i \sin\phi_i, \\ \dot{Y}_i &= \dot{x}_i \sin\phi_i + \dot{y}_i \cos\phi_i. \end{aligned} \quad (9)$$

Combining (6)-(9) and assuming that the longitudinal velocity can be regarded as a constant in (6) [18], the nonlinear lateral dynamics of follower vehicle i can be rewritten as

$$\dot{\xi}_{iy} = \Theta(\xi_{iy}, u_{iy}), \quad (10)$$

where $\xi_{iy} = [\dot{x}_i, \dot{y}_i, \phi_i, \dot{\phi}_i, \dot{X}_i, \dot{Y}_i]^\top$ and $u_{iy} = \delta_i$. The lateral discrete-time dynamics of vehicle i can be expressed as

$$\begin{aligned} \xi_{iy}(t+1) &= f_{iy}(\xi_{iy}(t), u_{iy}(t)) \\ &= \xi_{iy}(t) + \Delta t \Gamma_i(\xi_{iy}(t)) + \Delta t B_i u_{iy}(t), \end{aligned} \quad (11)$$

where

$$\Gamma_i(\xi_{iy}(t)) = \begin{bmatrix} 0 \\ -\frac{C_{ir}+C_{if}}{m_i\dot{x}_i}\dot{y}_i(t) - \left(\dot{x}_i + \frac{l_{if}C_{if} - l_{ir}C_{ir}}{m_i\dot{x}_i}\right)\dot{\phi}_i(t) \\ \dot{\phi}_i(t) \\ -\frac{l_{if}C_{if} - l_{ir}C_{ir}}{I_i\dot{x}_i}\dot{y}_i(t) - \frac{l_{if}^2 C_{if} + l_{ir}^2 C_{ir}}{I_i\dot{x}_i}\dot{\phi}_i(t) \\ \dot{x}_i(t)\cos\phi_i(t) - \dot{y}_i(t)\sin\phi_i(t) \\ \dot{x}_i(t)\sin\phi_i(t) + \dot{y}_i(t)\cos\phi_i(t) \end{bmatrix},$$

and $B = [0, \frac{C_{if}}{m_i}, 0, \frac{l_{if}C_{if}}{I_i}, 0, 0]^\top$. The lateral output is $\eta_{iy}(t) = \gamma_y \xi_{iy}(t) = [\phi_i(t), \dot{\phi}_i(t), Y_i(t)]^\top$, with $\gamma_y = \begin{bmatrix} 0,0,1,0,0,0 \\ 0,0,0,1,0,0 \\ 0,0,0,0,0,1 \end{bmatrix}$.

2.3 Platoon Control Objective

This paper is interested in longitudinal and lateral platoon control subject to a dynamic leader driven by a human driver. The longitudinal control objective is to track leader's speed $v_0(t)$ and maintain a constant distance d_0 between the consecutive vehicles. The lateral control objective is to track the lateral coordinate $Y_0(t)$ and the yaw angle $\phi_0(t)$ of the leader, and circumambulate the obstacles on the road while keeping the minimal gaps from other vehicles and the obstacles bigger than a safe constant. The longitudinal control objective can be formulated as

$$\lim_{t\to+\infty} \begin{cases} \|v_i(t) - v_0(t)\| = 0 \\ \|x_i(t) - x_0(t) + id_0\| = 0 \end{cases}. \quad (12)$$

Assume that there are M obstacles on the road and define $\mathcal{M} = \{1, 2, \ldots, M\}$. $\mathbb{X}_i$, $\mathbb{O}_m$ are the plane areas of vehicle i and obstacle m. Given the leader's lateral position Y_0 in global coordinate and yaw angle ϕ_0, the lateral control objective can be formulated as

$$\begin{cases} \lim\limits_{t\to+\infty} \|Y_i(t) - Y_0(t)\| = 0 \\ \lim\limits_{t\to+\infty} \|\phi_i(t) - \phi_0(t)\| = 0 \\ \mathbb{O}_m \cap \mathbb{X}_i(t) = \varnothing, m \in \mathcal{M} \\ \mathbb{X}_j(t) \cap \mathbb{X}_i(t) = \varnothing, j \in (\mathcal{N}_+ \cup \{0\}) \backslash \{i\} \end{cases}. \tag{13}$$

To easily describe the errors, define the longitudinal position error and lateral position error as $e_{ix}(t) = X_i(t) + id_0 - X_0(t)$ and $e_{iy}(t) = Y_i(t) - Y_0(t)$ respectively.

3 Hierarchical Distributed MPC Design

As shown in Fig. 1, we propose a hierarchical controller of each follower vehicle. The upper layer of follower i, $i \in \mathcal{N}_+$ will receive information from the predecessor $i-1$, and detect the environment. When there are external obstacles, the upper layer of vehicle i will plan a feasible path for it to avoid the obstacles. Based on the information from the predecessor $i-1$ and the planned path, a reference trajectory can be computed. The lower layer controller of vehicle i will control vehicle i to track the reference trajectory, keep the platoon, and avoid collisions.

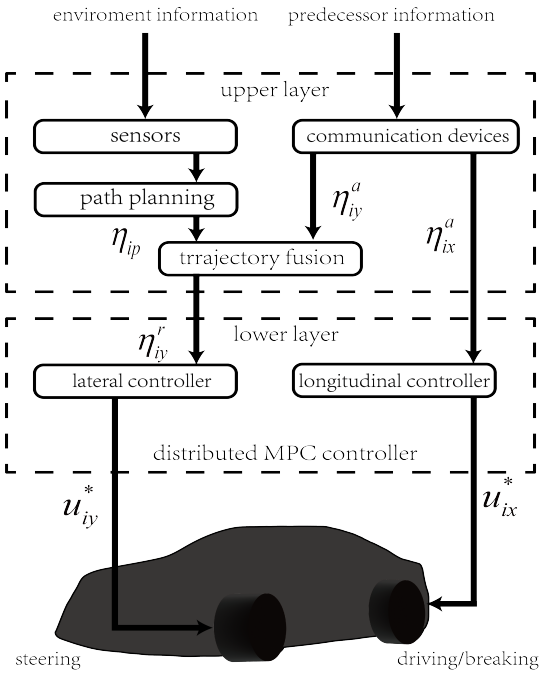

Fig. 1: Hierarchical control architecture

3.1 Longitudinal Control

Firstly, we define the same predictive horizon N_p for all vehicles and three types of state trajectories for follower i

$$\begin{array}{ll} \xi^p_{ix}(k|t),\ k = 0, 1, \ldots, N_p, & \text{Predicted state trajectory,} \\ \xi^a_{ix}(k|t),\ k = 0, 1, \ldots, N_p, & \text{Assumed state trajectory,} \\ \xi^*_{ix}(k|t),\ k = 0, 1, \ldots, N_p, & \text{Optimal state trajectory,} \end{array}$$

The output and control input will be defined in the same way.

In this paper, the predecessor-following (PF) communication topology is adopted. Then the local longitudinal optimization problem for follower i is formulated as

Problem 3.1. *for $i = 1, 2, \ldots, N$, $j = i - 1$:*

$$\min_{u^p_{ix}(\cdot|t)} J_{ix}(\eta^p_{ix}(\cdot|t), \eta^a_{ix}(\cdot|t), \eta^a_{jx}(\cdot|t), u^p_{ix}(\cdot|t)), \tag{14a}$$

$$s.t. \forall k = 0, 1, 2, \ldots, N_p - 1,$$

$$\xi^p_{ix}(k+1|t) = f_{ix}(\xi^p_{ix}(k|t), u^p_{ix}(k|t)), \tag{14b}$$

$$\eta^p_{ix}(k|t) = \gamma_x \xi^p_{ix}(k|t), \tag{14c}$$

$$\xi^p_{ix}(0|t) = \xi_{ix}(t), \tag{14d}$$

$$v^p_i(k|t) \in \mathbb{V}_i, \tag{14e}$$

$$u^p_{ix}(k|t) \in \mathbb{U}_{ix}, \tag{14f}$$

$$x^a_j(k|t) - x^p_i(k|t) \geq d_{safe}, \tag{14g}$$

$$\eta^p_i(N_p|t) = \eta^a_j(N_p|t) - [d_0, 0]^\top, \tag{14h}$$

$$T^p_i(N_p|t) = \frac{R_i m_i g \mu_i}{\eta_{T,i}}, \tag{14i}$$

where (14h)*,* (14i) *are the terminal constraints that ensure the string stability [11].*

The cost function (14a) is defined as

$$\begin{aligned} &J_{ix}(\eta^p_{ix}(\cdot|t), \eta^p_{jx}(\cdot|t), \eta^a_{jx}(\cdot|t), u^p_{ix}(\cdot|t)) \\ &= \sum_{k=0}^{N_p-1} (\|\eta^p_{ix}(k|t) - \eta^a_{ix}(k|t)\|_{G_{ix}} \\ &\quad + \|u^p_{ix}(k|t) - \frac{R_i m_i g \mu_i}{\eta_{T,i}}\|_{H_{ix}} \\ &\quad + \|\eta^p_{ix}(k|t) - \eta^a_{jx}(k|t)\|_{W_i}), \end{aligned} \tag{15}$$

where $G_{ix} \in \mathbb{R}^2$, $W_i \in \mathbb{R}^2$ are both symmetric positive-define matrices and $H_{ix} \in \mathbb{R}$ is a positive coefficient.

By solving Problem 3.1, the optimal input trajectory $u^*_{ix}(\cdot|t)$ and optimal output trajectory $\eta^*_{ix}(\cdot|t)$ at time t can be obtained.

Then the assumed input $u^a_{ix}(\cdot|t+1)$ of vehicle i for time $t+1$ can be computed as

$$u^a_{ix}(k|t+1) = \begin{cases} u^*_{ix}(k+1|t), k = 0, 1, \ldots, N_p - 2 \\ \frac{R_i m_i g \mu_i}{\eta_{T,i}}, k = N_p - 1 \end{cases}, \tag{16}$$

then the assumed state and output trajectories for time $t+1$ can be calculated as

$$\begin{aligned} \xi^a_{ix}(k+1|t+1) &= f_{ix}(\xi^a_{ix}(k|t+1), u^a_{ix}(k|t+1)), \\ \eta^a_{ix}(k|t+1) &= \gamma_x \xi^a_{ix}(k|t+1). \end{aligned} \tag{17}$$

3.2 Lateral Control with Collision Avoidance Constraints

Each follower i, $i \in \mathcal{N}_+$ requires to avoid the collision with the predecessor vehicle $i-1$ and the obstacles on the road to ensure safety. We define the safe reference trajectory for each follower i computed by the upper layer as $\eta^r_{iy} = [\phi^r_i, \dot{\phi}^r_i, Y^r_i]$. The MPC optimization problem for lateral control can be formulated as

Problem 3.2. *for $i = 1, 2, \ldots, N$, $j = i - 1$:*

$$\min_{u_{iy}^p(\cdot|t)} J_{iy}(\eta_{iy}^p(\cdot|t), \eta_{iy}^r(\cdot|t), u_{iy}^p(\cdot|t)), \tag{18a}$$

$$s.t. \forall k = 0, 1, 2, \ldots, N_p - 1,$$

$$\xi_{iy}^p(k+1|t) = f_{iy}(\xi_{iy}^p(k|t), u_{iy}^p(k|t)), \tag{18b}$$

$$\eta_{iy}^p(k|t) = \gamma_y \xi_{iy}^p(k|t), \tag{18c}$$

$$\xi_{iy}^p(0|t) = \xi_{iy}(t), \tag{18d}$$

$$u_{iy}^p \in \mathbb{U}_{iy}, \tag{18e}$$

$$\mathbb{X}_i^p(k|t) \cap \mathbb{X}_j^a(k|t) = \varnothing \tag{18f}$$

$$\mathbb{X}_i^p(k|t) \cap \mathbb{O}_m = \varnothing, \ \forall m \in \mathcal{M}. \tag{18g}$$

where $\mathbb{U}_{iy}$ is the lateral input constraint.

The cost function (18a) is chosen as

$$\begin{aligned} &J_{iy}(\eta_{iy}^p(\cdot|t), \eta_{iy}^r(\cdot|t), u_{iy}^p(\cdot|t)) \\ &= \sum_{k=0}^{N_p} \|\eta_{iy}^p(k|t) - \eta_{iy}^r(k|t)\|_{G_{iy}} + \sum_{k=0}^{N_p-1} \|u_{iy}^p(k|t)\|_{H_{iy}} + \rho\epsilon^2, \end{aligned} \tag{19}$$

where $G_{iy} \in \mathbb{R}^3$ is symmetric positive-define matrix and $H_{iy} \in \mathbb{R}$, $\rho \in \mathbb{R}$ are positive coefficients; ϵ is a relaxation factor to ensure the feasibility of Problem 3.2 [15].

The reference trajectory $\eta_{iy}^r(\cdot|t)$ in Problem 3.2 is computed by the upper layer at time t, and it must avoid collisions. However, the lower controller can not always follow the reference trajectory without tracking errors. Hence constraints (18f) and (18g) are introduced to ensure safety. However, constraints like (18f) are nested with other optimization problems which leads to heavy calculation burden of Problem 3.2. Next, the collision avoidance constraints (18f) and (18g) will be reformulated.

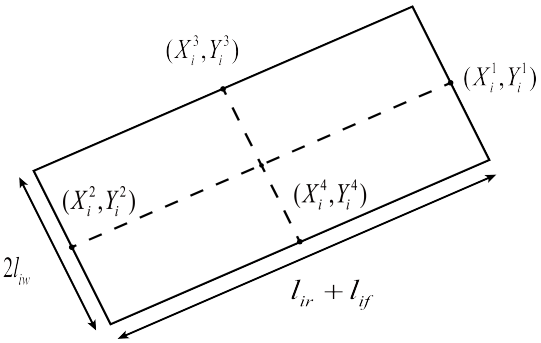

Fig. 2: Convex over-approximation of vehicle i

As shown in Fig. 2, given l_{iw} as the width of vehicle i, the convex over-approximation of vehicle i can be given as [19]

$$\mathbb{D}_i = \{p \in \mathbb{R}^2 : Q_i p \leq q_i\}, \tag{20}$$

$$Q_i = \begin{bmatrix} \cos\phi_i & \sin\phi_i \\ -\cos\phi_i & -\sin\phi_i \\ -\sin\phi_i & \cos\phi_i \\ \sin\phi_i & -\cos\phi_i \end{bmatrix}, \tag{21}$$

$$q_i = \begin{bmatrix} X_i^1 \cos\phi_i + Y_i^1 \sin\phi_i \\ -X_i^2 \cos\phi_i - Y_i^2 \sin\phi_i \\ -X_i^3 \sin\phi_i + Y_i^3 \cos\phi_i \\ X_i^4 \sin\phi_i - Y_i^4 \cos\phi_i \end{bmatrix}. \tag{22}$$

Similarly, the obstacles can be approximated as

$$\mathbb{O}_m = \{p \in \mathbb{R}^2 : A_m p \leq b_m\}. \tag{23}$$

Collision avoidance constraints (18f)-(18g) can be rewritten as

$$dist(\mathbb{X}_i(k|t), \mathbb{O}_m) \geq d_{min}, \ m \in \mathcal{M}, \tag{24}$$

$$dist(\mathbb{X}_i(k|t), \mathbb{X}_j(k|t)) \geq d_{min}, \ j = i - 1, \tag{25}$$

where $dist(\mathbb{X}_i(k|t), \mathbb{O}_m) = \min_r\{\|r\| : (\mathbb{X}_i(k|t) \bigoplus r) \cap \mathbb{O}_m \neq \varnothing\}$ and $dist(\mathbb{X}_i(k|t), \mathbb{X}_j(k|t)) = \min_r\{\|r\| : (\mathbb{X}_i(k|t) \bigoplus r) \cap \mathbb{X}_j(k|t) \neq \varnothing\}$. Considering the lateral position, d_{min} denotes the minimal safe distance which is different from d_{safe}. The reformulation of collision avoidance constraints can be given as follows.

Proposition 1. *[19, 20] The constraint* (24) *holds, if $\forall m \in \mathcal{M}$ there exist $\lambda_{i,m}(k|t)$, $\nu_{i,m}(k|t)$ satisfying*

$$\begin{aligned} -q_i^\top(k|t)\nu_{i,m}(k|t) - b_i^\top \lambda_{i,m}(k|t) &\geq d_{min}, \\ Q_i^\top(k|t)\nu_{i,m}(k|t) + A_m^\top \lambda_{i,m}(k|t) &= 0, \\ \lambda_{i,m}(k|t) \succeq 0, \nu_{i,m}(k|t) &\succeq 0, \\ \|A_m^\top \lambda_{i,m}(k|t)\|_* &\leq 1. \end{aligned} \tag{26}$$

The constraint (25) can be addressed similarly and Problem 3.2 is transformed into Problem 3.3.

Problem 3.3. *for $i = 1, 2, \ldots, N$, $j = i - 1$:*

$$\min_{u_{iy}^p(\cdot|t), \nu_{i,m}(\cdot|t), \lambda_{i,m}(\cdot|t), \nu_{i,j}(\cdot|t), \lambda_{i,j}(\cdot|t)} J_{iy}, \tag{27a}$$

$$s.t. \forall k = 0, 1, 2, \ldots, N_p - 1,$$

$$\xi_{iy}^p(k+1|t) = f_{iy}(\xi_{iy}^p(k|t), u_{iy}^p(k|t)), \tag{27b}$$

$$\eta_{iy}^p(k|t) = \gamma_y \xi_{iy}^p(k|t), \tag{27c}$$

$$\xi_{iy}^p(0|t) = \xi_{iy}(t), \tag{27d}$$

$$u_{iy}^p \in \mathbb{U}_{iy}, \tag{27e}$$

$$-q_i^\top(k|t)\nu_{i,m}(k|t) - b_i^\top \lambda_{i,m}(k|t) \geq d_{min}, \tag{27f}$$

$$-q_i^\top(k|t)\nu_{i,j}(k|t) - q_j^\top(k|t)\lambda_{i,j}(k|t) \geq d_{min}, \tag{27g}$$

$$Q_i^\top(k|t)\nu_{i,m}(k|t) + A_m^\top \lambda_{i,m}(k|t) = 0, \tag{27h}$$

$$Q_i^\top(k|t)\nu_{i,j}(k|t) + Q_j^\top(k|t)\lambda_{i,j}(k|t) = 0, \tag{27i}$$

$$\|A_m^\top \lambda_{i,m}(k|t)\|_* \leq 1, \tag{27j}$$

$$\|Q_j^\top(k|t)\lambda_{i,j}(k|t)\|_* \leq 1, \tag{27k}$$

$$\lambda_{i,m}(\cdot|t) \succeq 0, \nu_{i,m}(\cdot|t) \succeq 0 \tag{27l}$$

$$\lambda_{i,j}(\cdot|t) \succeq 0, \nu_{i,j}(\cdot|t) \succeq 0 \tag{27m}$$

where $Q_j(\cdot|t)$ and $q_j(\cdot|t)$ are the assumed area occupied by vehicle j computed using the assumed state trajectory $\xi_{iy}^a(\cdot|t)$ of vehicle j.

3.3 Design of Upper Layer

In this subsection, a new constructive vector field method is adopted for path planning. Unlike the conditional artificial potential field method, the sharp steering that may make Problem 3.3 infeasible can be avoided [21].

Consider the position $p_i \in \mathbb{R}^2$ in global coordinate of vehicle i and a time-varying curve $\mathcal{C}(t) \in \mathbb{R}^2$. The goal is

to find the vector field that guides the position p_i converging to the objective curve $\mathcal{C}(t)$. Firstly, find the closest point p^* from the vehicle position p_i in the curve $\mathcal{C}(t)$ at time t. Then calculate the Euclidean vector $\mathbf{D}(p_i,t)$ and its norm

$$\begin{aligned}\mathbf{D}(p_i,t) &= p_i - p^*,\\ D(p_i,t) &= \|\mathbf{D}(p_i,t)\|.\end{aligned} \tag{28}$$

After that, define the unit tangent vector of the curve at point p^* as $\mathbf{T}(p^*,t)$. It should be noted that $\mathbf{D}^\top(p_i,t)\mathbf{T}(p^*,t) = 0$. The gains $G(p_i,t)$ and $H(p_i,t)$ of vectors $\mathbf{D}(p_i,t)$ and $\mathbf{T}(p^*,t)$ can be calculated respectively as

$$\begin{aligned}G(p_i,t) &= \frac{2}{\pi}\arctan k_G D(p_i,t),\\ H(p_i,t) &= \sqrt{1-(G(p_i,t))^2},\end{aligned} \tag{29}$$

where k_G is a positive constant. Next, the static and dynamic components in the attractive vector field of curve $\mathcal{C}(t)$ can be represented as

$$\begin{aligned}\mathbf{\Phi}_S(p_i,t) &= -G(p_i,t)\frac{\mathbf{D}(p_i,t)}{D(p_i,t)} + H(p_i,t)\mathbf{T}(p^*,t),\\ \mathbf{\Phi}_T(p_i,t) &= -\Pi_T\frac{\partial \mathbf{D}(p_i,t)}{\partial t},\end{aligned} \tag{30}$$

where Π_T is the null space projection matrix of $\mathbf{T}^*(p,t)$. Defining the constant stepper velocity v_r and ignoring (p_i,t) in description, then the gain κ can be calculate as

$$\kappa = -\mathbf{\Phi}_S\mathbf{\Phi}_T + \sqrt{(\mathbf{\Phi}_S\mathbf{\Phi}_T)^2 + v_r^2 - \|\mathbf{\Phi}_T\|^2}, \tag{31}$$

where $\|\mathbf{\Phi}\| = v_r$ can be achieved by the computation of κ. Finally, the attractive vector $\mathbf{\Phi}(p_i,t)$ can be obtained as

$$\mathbf{\Phi}(p_i,t) = \kappa(p_i,t)\mathbf{\Phi}_S(p_i,t) + \mathbf{\Phi}_T(p_i,t). \tag{32}$$

Supposed that an obstacle $\mathbb{O}_1$ is detected, find the closest point p_o^* in $\mathbb{O}_1$ from the vehicle position p_i. The Euclidean vector can be calculated as

$$\begin{aligned}\mathbf{D}_o(p_i,t) &= p_i - p_o^*,\\ D_o(p_i,t) &= \|\mathbf{D}_o(p_i,t)\|.\end{aligned} \tag{33}$$

To satisfy the collision avoidance constraints (27f)-(27m), a constant distance $l_{io} > 0$ is defined such that

$$l_{io} \geq d_{min} + \max\left\{\sqrt{l_{if}^2 + l_{iw}^2}, \sqrt{l_{ir}^2 + l_{iw}^2}\right\}. \tag{34}$$

The new Euclidean vector can be calculated as

$$\begin{aligned}\mathbf{D}_{l_{io}}(p_i,t) &= \mathbf{D}_o(p_i,t) - l_{io}\frac{\mathbf{D}_o(p_i,t)}{D_o(p_i,t)},\\ D_{l_{io}}(p_i,t) &= \|\mathbf{D}_{l_{io}}(p_i,t)\|,\end{aligned} \tag{35}$$

Then the circumambulating path can be obtained:

$$\mathcal{C}_o = \{p \in \mathbb{R}^2 : D(p,t) = l_{io}\}. \tag{36}$$

Next, by applying (28)-(32) to $\mathcal{C}_o$, the attractive vector $\mathbf{\Psi}(p_i,t)$ relative to obstacle $\mathbb{O}_1$ can be obtained. Define two distance parameters D_{in} and D_{in}^0 ($D_{in}^0 > D_{in} > l_{io}$), and the weight parameter can be obtained as

$$\theta(p_i,t) \equiv \theta = \frac{D_o(p_i,t) - D_{in}}{D_{in}^0 - D_{in}}. \tag{37}$$

Utilizing the attractive vectors $\mathbf{\Phi}(p_i,t)$ and $\mathbf{\Psi}(p_i,t)$, the whole constructive vector $\mathcal{F}$ can be formulated as

$$\mathcal{F} = \begin{cases}\mathbf{\Phi}, & \text{if } \mathbf{D}_0^\top\mathbf{\Phi} \geq 0 \text{ or } D_o > D_{in}^0\\ \mathbf{\Psi}, & \text{if } \mathbf{D}_0^\top\mathbf{\Phi} < 0, D_o < D_{in}\\ v_r\frac{\theta\mathbf{\Phi}+(1-\theta)\mathbf{\Psi}}{\|\theta\mathbf{\Phi}+(1-\theta)\mathbf{\Psi}\|}, & \text{else}\end{cases}. \tag{38}$$

Based on the constructive vector $\mathcal{F}$ in (38), the path planning algorithm is proposed as follows.

Algorithm 1 Path Planning Algorithm Based on Constructive Vector Field $\mathcal{F}$

Input: the global position p_i of follower i, midline of the road $\mathcal{C}$, obstacles $\mathbb{O}_m, m \in \mathcal{M}$, detective distance D_{det}, D_{in}^0, D_{in}

Output: a safe trajectory η_{ip} without collision

```
define empty set η_ip, and let p = p_i;
while 𝕆_m ∩ (p ⊕ D_det) ≠ ∅ do
    calculate Φ, Ψ;
    calculate F;
    calculate yaw angle and yaw rate φ_p, φ̇_p;
    store the state point in η_ip;
    p ← p + F;
end while
```

In this paper, each follower vehicle i has two tasks, that is, following the predecessor vehicle to maintain platoon formation, and following the planned path to avoid collision if there exist obstacles. However, there may well be a conflict between the trajectory from the predecessor vehicle and the local planned path. To avoid abrupt transitions caused by the conflict, a new trajectory is constructed by fusing the trajectory from the predecessor vehicle $i-1$ and the local planned trajectory. Define the distances D_{on}^0 and D_{on} satisfying $D_{in}^0 \leq D_{on} < D_{on}^0 \leq D_{det}$. The fusion coefficient is defined as

$$\beta_i = \frac{D_o(p_i,t) - D_{on}}{D_{on}^0 - D_{on}}. \tag{39}$$

Then the fused reference trajectory given to lower-layer controller is constructed as

$$\eta_{iy}^r(k|t) = \begin{cases}\eta_{jy}^a(k|t), & D_o > D_{on}^0\\ \eta_{ip}(k|t), & D_o < D_{on}\\ \beta_i\eta_{iy}^a + (1-\beta_i)\eta_{ip}, & \text{else}\end{cases}, \tag{40}$$

where $\eta_{iy}^a(k|t)$ is constructed in the same way as (16)-(17).

3.4 Hierarchical Distributed MPC Design

We assume that the assumed output of leader is available. Based on subsections 3.1- 3.3, the whole hierarchical control architecture is summarized below.

Algorithm 2 Hierarchical Distributed MPC for Longitudinal and Lateral Vehicle Platoon Control with Collision Avoidance

Input: the platoon operating stably at $t = 0$ and no obstacles detected at $t = 0$;

Initialization: $\forall$ follower $i(i \in \mathcal{N}_+)$:
longitudinal assumed control input is set as $u^a_{ix}(\cdot|t) = 0$;
calculate longitudinal assumed output as (17);
the lateral output is set as $\eta^a_{iy}(\cdot|t) = 0$;
send $\eta^a_{ix}(\cdot|t), \eta^a_{iy}(\cdot|t)$ to follower $i + 1$;
Iteration: $\forall$ follower $i(i \in \mathcal{N}_+)$:
while $t > 0$ **do**
    detect the environment and sample the state $\xi_{ix}(t)$ and $\xi_{iy}(t)$;
    plan the trajectory by Algorithm 1;
    construct reference trajectory with (40);
    solve Problem 3.1 and Problem 3.3 with $\xi_{ix}(t)$, $\xi_{iy}(t)$ and obtain $u^*_{ix}(\cdot|t)$, $u^*_{iy}(\cdot|t)$;
    construct assumed output $\eta^a_{ix}(\cdot|t+1)$, $\eta^a_{iy}(\cdot|t+1)$;
    send $\eta^a_{ix}(\cdot|t+1)$ and $\eta^a_{iy}(\cdot|t+1)$ to follower $i + 1$;
    control follower i using $u^*_{ix}(0|t)$, $u^*_{iy}(0|t)$;
    $t \leftarrow t + 1$;
end while

4 Simulation Results

The effectiveness of the proposed Algorithm 2 is demonstrated by a numerical simulation. Consider a platoon with a leader vehicle and 3 follower vehicles. Other simulation parameters are given in Table 1.

Table 1: Parameters of the Follower Vehicles

Parameters	Values	Parameters	Values
v_0	10	$\eta_{T,i}$	0.85
d_{safe}	5	Δt	0.1
d_0	20	N_p	21
τ_i	0.075	G_{ix}	$\begin{bmatrix} 10 & 0 \\ 0 & 10 \end{bmatrix}$
μ_i	0.015	H_{ix}	1
m_i	2500	W_i	$\begin{bmatrix} 10 & 0 \\ 0 & 10 \end{bmatrix}$
I_i	5000	G_{iy}	$\begin{bmatrix} 20 & 0 & 0 \\ 0 & 8 & 0 \\ 0 & 0 & 22 \end{bmatrix}$
C_{if}	20000	H_{iy}	1
C_{ir}	20000	ρ_i	1600
l_{if}	2.3	d_{min}	0.5
l_{ir}	2.1	D_{in}	8
l_{iw}	1	D^0_{in}	15
R_i	0.35	D_{on}	40
D^0_{on}	60		

The leader is driving straightly on the middle line of the road, that is $Y_0 = 0$, and all followers are driving with $e_{iy} = 0.7m$. Besides, there exists a rectangle obstacle on global coordinate $(23, 0)$. The obstacle's length is $8m$ and its width is $2m$.

We use a path tracking algorithm to imitate the human-driven leader vehicle. Fig. 3 shows the state trajectories of the vehicles in platoon under the control of Algorithm 2. In Fig. 3(b), the velocities are kept at about v_0 when the followers regulate steering angles and converge to v_0 after the regulation. In Fig. 3(c), the yaw angle of follower 2 varies faster than the yaw angle of follower 1 but slower than the yaw angle of follower 3 in the first $2s$, which indicates that

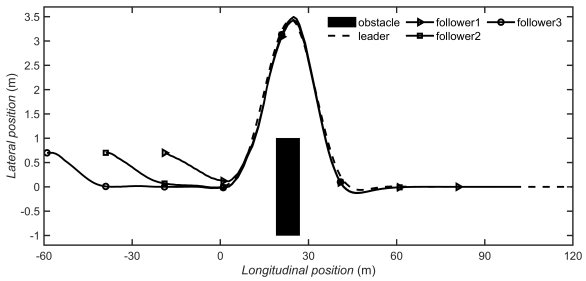

(a) Position trajectories

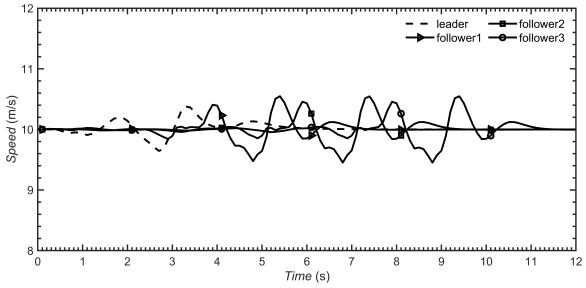

(b) Velocities

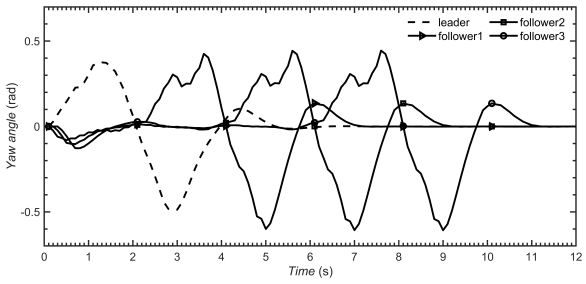

(c) Yaw angles

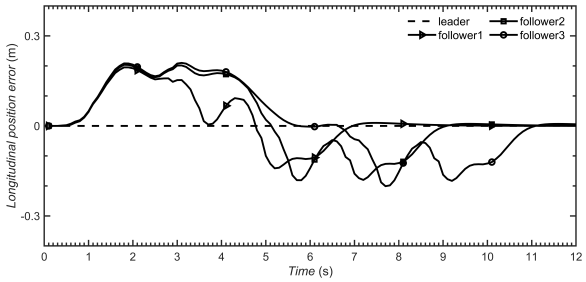

(d) Longitudinal position errors

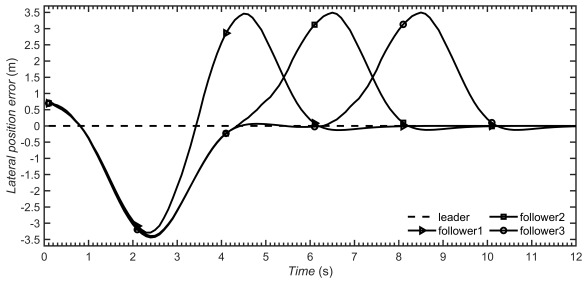

(e) Lateral position errors

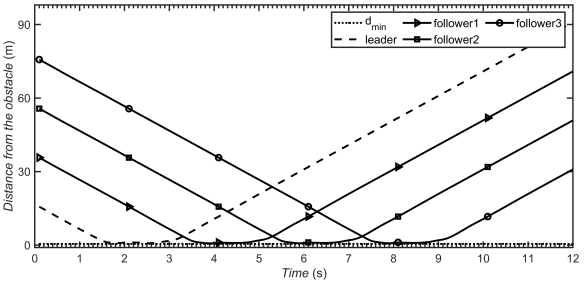

(f) Distance from obstacle

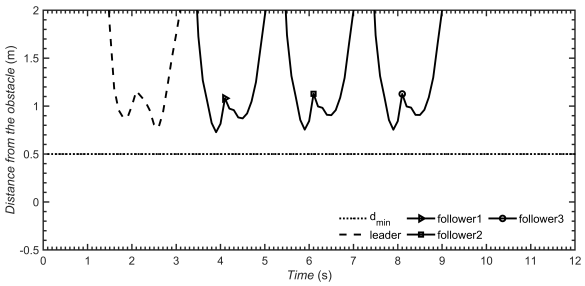

(g) Distance from obstacle (enlarged)

Fig. 3: 2-dimensional scenario with obstacle and lateral position errors

our trajectory-fusion method gives a good transition. Fig. 3(a) shows the position trajectory of each vehicle. The followers steer firstly to avoid the obstacle and finally they follow the leader with no longitudinal position errors (see Fig. 3(d)) and no lateral position errors (see Fig. 3(e)). As shown in Fig. 3(f)-3(g), the minimal distances from the obstacle are always bigger than d_{min}, which indicates that our collision avoidance constraints keep working in the simulation. Based on the results, the control objectives (12) and (13) are achieved.

5 Conclusions

This paper proposes a novel hierarchical distributed MPC method for longitudinal and lateral control of the vehicle platoon. The objective of each follower vehicle in the platoon is to track the velocity, longitudinal position, yaw angle and lateral position of the leader vehicle while keeping a safe gap from the predecessor vehicle and circumambulating obstacles on the road. The dynamics of each follower vehicle is decoupled in longitudinal and lateral directions. If no obstacle is detected, our controller is able to track the velocity and lateral position of leader while keeping a constant inter-vehicle distance in the platoon. If there exist some obstacles, the followers will construct a feasible and smooth trajectory to circumambulate the obstacles and converge to desired lateral position finally. Based on strong duality theory, the collision avoidance constraints can be reformulated to keep the platoon safe and avoid collisions.

References

[1] D. Jia, K. Lu, J. Wang, X. Zhang, and X. Shen, "A survey on platoon-based vehicular cyber-physical systems," *IEEE communications surveys & tutorials*, 18(1): 263–284, 2015.

[2] P. Xavier and Y.-J. Pan, "A practical pid-based scheme for the collaborative driving of automated vehicles," in *Proceedings of the 48h IEEE Conference on Decision and Control (CDC) held jointly with 2009 28th Chinese Control Conference*, : 966–971, IEEE, 2009.

[3] G. J. Naus, R. P. Vugts, J. Ploeg, M. J. van De Molengraft, and M. Steinbuch, "String-stable cacc design and experimental validation: A frequency-domain approach," *IEEE Transactions on vehicular technology*, 59(9): 4268–4279, 2010.

[4] V. Milanés, S. E. Shladover, J. Spring, C. Nowakowski, H. Kawazoe, and M. Nakamura, "Cooperative adaptive cruise control in real traffic situations," *IEEE Transactions on intelligent transportation systems*, 15(1): 296–305, 2013.

[5] X. Liu, A. Goldsmith, S. S. Mahal, and J. K. Hedrick, "Effects of communication delay on string stability in vehicle platoons," in *ITSC 2001. 2001 IEEE Intelligent Transportation Systems. Proceedings (Cat. No. 01TH8585)*, : 625–630, IEEE, 2001.

[6] J. Zhao, M. Oya, and A. El Kamel, "A safety spacing policy and its impact on highway traffic flow," in *2009 IEEE Intelligent Vehicles Symposium*, : 960–965, IEEE, 2009.

[7] K. C. Dey, L. Yan, X. Wang, Y. Wang, H. Shen, M. Chowdhury, L. Yu, C. Qiu, and V. Soundararaj, "A review of communication, driver characteristics, and controls aspects of cooperative adaptive cruise control (cacc)," *IEEE Transactions on Intelligent Transportation Systems*, 17(2): 491–509, 2015.

[8] W. B. Dunbar and R. M. Murray, "Distributed receding horizon control for multi-vehicle formation stabilization," *Automatica*, 42(4): 549–558, 2006.

[9] W. B. Dunbar, "Distributed receding horizon control of dynamically coupled nonlinear systems," *IEEE Transactions on Automatic Control*, 52(7): 1249–1263, 2007.

[10] R. Kianfar, P. Falcone, and J. Fredriksson, "A receding horizon approach to string stable cooperative adaptive cruise control," in *2011 14th International IEEE Conference on Intelligent Transportation Systems (ITSC)*, : 734–739, IEEE, 2011.

[11] Y. Zheng, S. E. Li, K. Li, F. Borrelli, and J. K. Hedrick, "Distributed model predictive control for heterogeneous vehicle platoons under unidirectional topologies," *IEEE Transactions on Control Systems Technology*, 25(3): 899–910, 2016.

[12] S. E. Shladover, C. A. Desoer, J. K. Hedrick, M. Tomizuka, J. Walrand, W.-B. Zhang, D. H. McMahon, H. Peng, S. Sheikholeslam, and N. McKeown, "Automated vehicle control developments in the path program," *IEEE Transactions on vehicular technology*, 40(1): 114–130, 1991.

[13] D. Jia and D. Ngoduy, "Enhanced cooperative car-following traffic model with the combination of v2v and v2i communication," *Transportation Research Part B: Methodological*, 90: 172–191, 2016.

[14] Y. Li, W. Chen, S. Peeta, and Y. Wang, "Platoon control of connected multi-vehicle systems under v2x communications: design and experiments," *IEEE Transactions on Intelligent Transportation Systems*, 21(5): 1891–1902, 2019.

[15] S. Wei, Y. Zou, X. Zhang, T. Zhang, and X. Li, "An integrated longitudinal and lateral vehicle following control system with radar and vehicle-to-vehicle communication," *IEEE Transactions on Vehicular Technology*, 68(2): 1116–1127, 2019.

[16] M. Floren, A. Khajepour, and E. Hashemi, "An integrated control approach for the combined longitudinal and lateral vehicle following problem," in *2021 American Control Conference (ACC)*, : 436–441, IEEE, 2021.

[17] O. Pauca, C. F. Caruntu, and C. Lazar, "Predictive control for the lateral and longitudinal dynamics in automated vehicles," in *2019 23rd International Conference on System Theory, Control and Computing (ICSTCC)*, : 797–802, IEEE, 2019.

[18] R. Rajamani, *Vehicle dynamics and control*. Springer Science & Business Media, 2011.

[19] L. Dai, Y. Hao, H. Xie, Z. Sun, and Y. Xia, "Distributed robust mpc for nonholonomic robots with obstacle and collision avoidance," *Control Theory and Technology*, 20(1): 32–45, 2022.

[20] X. Zhang, A. Liniger, and F. Borrelli, "Optimization-based collision avoidance," *IEEE Transactions on Control Systems Technology*, 29(3): 972–983, 2020.

[21] A. H. Nunes, A. M. Rezende, G. P. Cruz, G. M. Freitas, V. M. Gonçalves, and L. C. Pimenta, "Vector field for curve tracking with obstacle avoidance," in *2022 IEEE 61st Conference on Decision and Control (CDC)*, : 2031–2038, IEEE, 2022.